Proceedings of ICRC 2001: 2014 © Copernicus Gesellschaft 2001

ICRC 2001

Energy spectrum and acceleration rate in relativistic shock acceleration

R. J. Protheroe

Department of Physics and Mathematical Physics, University of Adelaide, SA 5001, Australia

Abstract. In this paper I present Monte Carlo results for shock acceleration at an ultrarelativistic shock for the case where propagation downstream can be approximated by a random walk with isotropic scattering. An event generator for the downstream part of the cycle was developed and results in extremely efficient Monte Carlo simulation. Two simple scattering models are used upstream: isotropic scattering, and small angle scattering. The angular distribution of particles at the shock, and the distribution of momentum as a function of time after injection are given together with the resulting momentum spectrum of accelerated particles. The results for small angle scattering are in qualitative agreement with more sophisticated treatments.

1 Introduction

In relativistic shock acceleration the nature of scattering plays an important role in shaping the angular distribution of particles crossing the shock, and hence the acceleration rate and spectrum. The acceleration time scale and efficiency for various scattering models is discussed by Bednarz and Ostrowski (1996, 1999). For a recent review of relativistic shock acceleration see Ostrowski (2001).

In an accompanying paper (Protheroe 2001), I considered propagation propagation of particles downstream of a strong relativistic shock, i.e. Lorentz factor of shock in upstream frame $\Gamma_1 \gg 1$, moving through a relativistic plasma. In this case, the downstream flow velocity is $u_2 \approx c/3$. The shock geometry and an acceleration cycle are illustrated in fig. 1 of Protheroe (2001). Note that I use unprimed variables for the upstream frame, singly-primed variables for the downstream frame, and doubly-primed variables for the shock frame, and define the direction of flow in the shock frame to be in the positive x''-direction, and the shock to be at $x'' = 0$ ($x'' < 0$ is upstream and $x'' > 0$ is downstream).

The downstream part of the shock acceleration cycle is simulated quickly and efficiently by sampling $\cos\theta_2'$ from $p(\cos\theta_2'; \cos\theta_1')$, and t_d' from $p(t_d'; \cos\theta_2', \cos\theta_1')$ for a particle crossing from upstream to downstream at angle θ_1. These distributions are given by Protheroe (2001).

Correspondence to: rprother@physics.adelaide.edu.au

2 Simulation of motion upstream and acceleration

For the random walk, the mean free path I adopt downstream is $\lambda^{\rm sc}(p') = (p'/p_0')^\alpha \lambda_0^{\rm sc}$, and upstream I take $\lambda^{\rm sc}(p) = (Rp/p_0')^\alpha \lambda_0^{\rm sc}$ where $R = 4\Gamma_{12}$ is the compression ratio. For $\alpha = 1$ this is motivated by the Bohm diffusion case where the mean free path is proportional to the gyroradius, and by the magnetic field (which I assume to be tangled) being approximately a factor R larger downstream. I sample a path from an exponential distribution with mean $\lambda^{\rm sc}$, and then sample a new direction. Scattering in the downstream plasma is isotropic in the downstream frame. In the upstream plasma I consider two different cases: (a) isotropic scattering, and (b) scattering to a new direction sampled from a two-dimensional normal distribution with root mean square deflection equal to $1/\Gamma_1$ (i.e. typically the particle is scattered through angle $1/\Gamma_1$ in the upstream frame). Case (a) is unrealistic, but simple to implement and easy to check by comparing with simple calculations. Case (b), which I shall refer to as "small angle scattering", although still a simple approximation, is motivated by several studies (e.g. Gallant and Achterberg 1999) which show that this is of the right order of magnitude for scattering upstream.

At the shock, at time $t = 0$, I inject highly relativistic monoenergetic particles which are isotropic in the upstream frame and have upstream-frame momentum $p_0 = p_0'/\Gamma_{12}$. Thus, as observed in the downstream frame these injected particles have a range of initial momenta distributed up to $\sim 2p_0'$. All distances are measured in units of $\lambda_0^{\rm sc}$ and all times are measured in units of $t_0^{\rm sc} = \lambda_0^{\rm sc}/c$. A system of weights is used to make the simulation efficient. Injected particles are assigned initial weights $w = 1$.

Those particles traveling initially upstream undergo a ran-

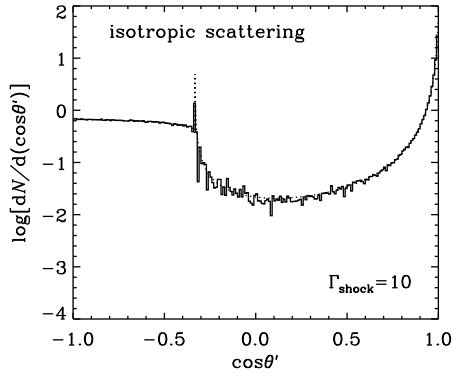

Fig. 1. Angular distribution of particles at the shock (histogram) for the case of isotropic scattering, compared with that expected (dotted curve) for $\Gamma_1 = 10$.

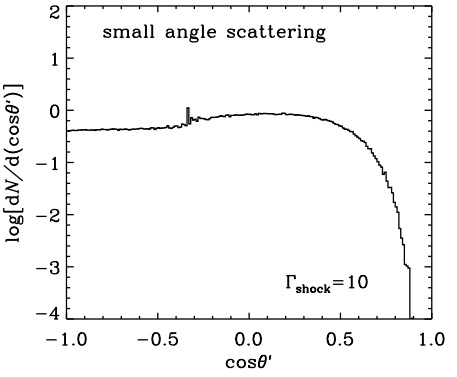

Fig. 2. Angular distribution of particles at the shock (histogram) for the case of small angle scattering for $\Gamma_1 = 10$.

dom walk upstream until the shock catches up with them. At that stage, their 4-positions and 4-momenta are Lorentz transformed to the downstream frame. Their directions, $\cos\theta_1'$, are recorded and binned (with weight w) to produce angular distributions of particles as they cross the shock. Similarly, their momenta, p', are recorded and used (with weight w) to update histograms of momenta of particles present in the system (i.e. not having escaped downstream) at discrete times since the last shock crossing.

A particle crossing from upstream to downstream at angle θ_1', has probability $P_r(\cos\theta_1') \equiv \mathrm{Prob.(return;}\cos\theta_1')$ of returning to the shock (see fig. 2 of Protheroe 2001). The histograms of momenta of particles which have escaped at time t' (and later times) are updated by adding $w[1 - P_r(\cos\theta_1')]$ to the appropriate momentum bins of each histogram. The particle then has its weight updated to $w = w_{\rm old}P_r(\cos\theta_1')$ and the direction on returning to the shock $\cos\theta_2'$ is sampled from the distribution $p(\cos\theta_2';\cos\theta_1')$ (see fig. 4 of Protheroe 2001). The time spent downstream is then updated by an amount sampled from the distribution $p(t_d';\cos\theta_2',\cos\theta_1')$ (see fig. 6 of Protheroe 2001) and multiplied by $(p'/p_0')^\alpha t_0^{\rm sc}$. The 4-positions and 4-momenta of the particles are updated to take account of their journeys downstream, and before the particles propagate upstream their directions, $\cos\theta_2'$, are binned (with weight w) to produce angular distributions of particles as they cross the shock from downstream to upstream. Similarly, their momenta, p', are recorded and used (with weight w) to update histograms of momenta of particles still present in the system since the last shock crossing.

3 Angular Distribution

Because of the simple scattering models adopted, the angular distributions are not expected to look like those for pitch-angle scattering given, e.g., by Kirk and Schneider (1987). However, it is straightforward to predict the angular distribution for the case of isotropic scattering, and use this as a check of the Monte Carlo simulation. In this case, the upstream-frame angular distribution of particles crossing from upstream to downstream is

$$p(\cos\theta;\,\mathrm{cross}) = (1+\beta_1)^{-1} \qquad (-\beta_1 < \cos\theta < 1),$$

giving $\langle\cos\theta\rangle_{\rm U\to D} \approx 0$. Lorentz transformation gives the downstream frame distribution for $-\beta_2 < \cos\theta' < 1$

$$p(\cos\theta';\,\mathrm{cross}) \;=\; \frac{(1-\beta_{12}^2)}{(1-\beta_{12}\cos\theta')^2(1+\beta_1)}.$$

The angular distribution of particles crossing from downstream to upstream ($-1 < \cos\theta' < -\beta_2$) is then

$$p(\cos\theta';\,\mathrm{cross}) \;=\; \int_{-\beta_2}^{1} p(\cos\theta_0';\,\mathrm{cross})\, P_r(\cos\theta_0')p(\cos\theta';\cos\theta_0')d\cos\theta_0',$$

from which I obtain $\langle\cos\theta'\rangle_{\rm D\to U} = -0.786$.

Particles traveling nearly parallel to the shock plane spend more time near the shock than particles traveling nearly perpendicular to the shock plane, thus

$$p(\cos\theta') \propto p(\cos\theta';\,\mathrm{cross})/(\cos\theta'+\beta_2).$$

The downstream angular distribution of particles at the shock is shown in Fig. 1 for the case of isotropic scattering where it is seen to be in excellent agreement with expectation. Fig. 2 shows the distribution for the case of isotropic scattering downstream and small angle scattering upstream (the spike at $\cos\theta' = -1/3$ is due to low statistics for particles travelling parallel to the shock plane).

4 Acceleration Rate

The average ratio of final to initial momentum by ultra-relativistic particles per acceleration cycle is

$$\frac{p_{n+1}'}{p_n'} = \Gamma_{12}^2(1+\beta_{12}\langle\cos\theta\rangle_{\rm U\to D})(1-\beta_{12}\langle\cos\theta'\rangle_{\rm D\to U}).$$

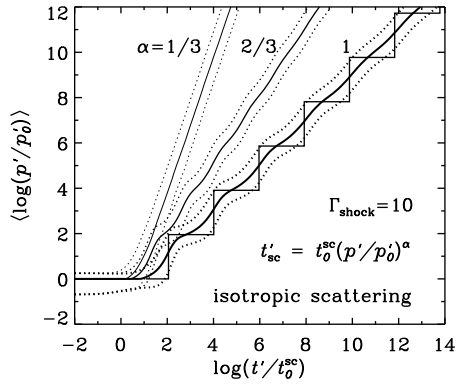

Fig. 3. Average value of $\log(p'/p'_0)$ ± 1 standard deviation vs. time since injection for the isotropic scattering case for the three p-dependences of the scattering mean free path for $\Gamma_1 = 10$ and (b) $\Gamma_1 = 20$. Also shown is a result obtained from simple theory (stepped curve) for the case of $\alpha = 1$.

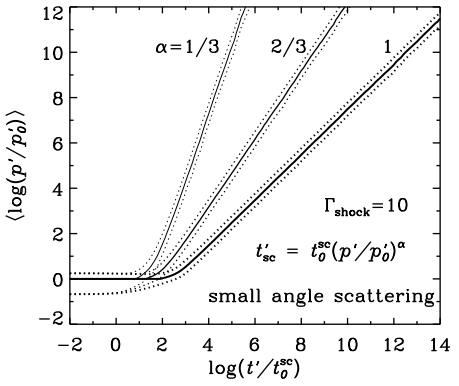

Fig. 4. Average value of $\log(p'/p'_0)$ ± 1 standard deviation vs. time since injectionfor the small angle scattering case for the three p-dependences of the scattering mean free path for $\Gamma_1 = 10$ and (b) $\Gamma_1 = 20$.

Again, in order to check the Monte Carlo results, I shall consider the isotropic scattering case, and using $\langle \cos\theta \rangle_{\mathrm{U}\to\mathrm{D}}$ and $\langle \cos\theta' \rangle_{\mathrm{D}\to\mathrm{U}}$ obtained above for this case, I find $p'_{n+1}/p'_n \approx 0.9\Gamma_1^2$, and this is within 25% of the result of Bednarz and Ostrowskii (1999) for the case of large magnetic field fluctuations. In the case of the small angle scattering, p'_{n+1}/p'_n will be very much lower, typically between 1 and 2 (e.g. Gallant and Achterberg 1999).

The average time per acceleration cycle is the average time spent downstream and upstream. For the case of isotropic scattering, both upstream and downstream, the downstream time is given approximately by $\langle t'_d \rangle \approx \langle t'_d(1) \rangle (p'/p'_0)^\alpha$ since in this case the distribution of particles crossing from upstream to downstream is strongly peaked at $\cos\theta' = 1$, giving $\langle t'_d \rangle \approx 4.2(p'/p'_0)^\alpha t_0^{\mathrm{sc}}$ (see fig. 5 of Protheroe 2001).

Particles crossing from downstream to upstream have an upstream velocity component parallel to the shock direction which is larger than the shock velocity, and therefore the shock will not overtake a particle until it scatters. In the case of isotropic scattering upstream, one scattering is usually sufficient for this to occur, and so the shock will have to travel typically $\Delta x \approx -\lambda^{\mathrm{sc}}(p)\cos\theta$ to catch up with the particle. The time spent upstream is then $\Delta t \approx -\lambda^{\mathrm{sc}}(p)\cos\theta/\beta_1$, and transformed to the downstream frame this becomes

$$\Delta t' = -\Gamma_{12}[(1-\Gamma_{12}\beta_{12}\cos\theta')R]^\alpha \left(\frac{\cos\theta'-\beta_{12}}{1-\beta_{12}\cos\theta'}\right)\left(\frac{1}{\beta_1}-\beta_{12}\right)\left(\frac{p'}{p'_0}\right)^\alpha t_0^{\mathrm{sc}}.$$

I obtain the average time spent upstream (isotropic scattering case) from

$$\langle t'_u \rangle = \frac{\int_{-\beta_2}^1 \Delta t'(\cos\theta') P_r(\cos\theta') d\cos\theta'}{\int_{-\beta_2}^1 P_r(\cos\theta') d\cos\theta'}$$

and for $\alpha = 1$ and $\Gamma_1 = 10$, I obtain $\langle t'_u \rangle = 19.6 t_0^{\mathrm{sc}}$, giving $p'_{n+1}/p'_n = 90$ and $\langle t'_{\mathrm{cycle}} \rangle = 23.8(p'/p'_0)$. I can plot on a graph of p' vs. t' points representing p'_{n+1} and their corresponding times $t'_{n+1} = t'_n + 23.8(p'_{n+1}/2p'_0)$ (taking the average momentum during the cycle). This is shown in Fig. 3 for $\alpha = 1$ and $\Gamma_1 = 10$ as the stepped curve. Results from the Monte Carlo simulation are also shown for $\alpha = 1/3$, $\alpha = 2/3$ and $\alpha = 1$, and in this latter case are seen to in good agreement with the approximate result. The rate of momentum gain for the case of Bohm diffusion with $\lambda^{\mathrm{sc}} = r_{\mathrm{gyro}}$ is $dp'/dt' \sim 0.1eB'c$ (i.e. $\sim$10% of the maximum for a given magnetic field). Fig. 4 shows results for small angle scattering upstream, and we see that the acceleration rate is considerably lower, about 0.5% of the maximum, and the fluctuations in energy at a given time after injection are much less.

5 Spectrum

For the case of isotropic scattering upstream, I estimate the spectral index from the momentum gain per cycle and the probability of escape downstream per cycle, as a further consistency check of the Monte Carlo simulation. To do this, I consider the generation of the momentum spectrum as a series of jumps in momentum from one "momentum level" to another. At each jump, the particle has a probability of reaching the next level given by

$$P_R = \int_{-\beta_2}^1 p(\cos\theta';\,\mathrm{cross}) P_r(\cos\theta') d\cos\theta' \approx P_r(1),$$

i.e. $P_R \approx 0.195$ (see fig. 2 of Protheroe 2001) which is marginally consistent with the result of Bednarz and Ostrowskii (1999) for the case of large magnetic field fluctuations (my result is about 50% higher, and this could be due to my use of isotropic scattering instead of following particle orbits in a random field).

Defining the ratio of final to initial momentum per acceleration cycle to be $a \equiv p'_{n+1}/p'_n$ ($a = 90$ for $\Gamma_1 = 10$ and

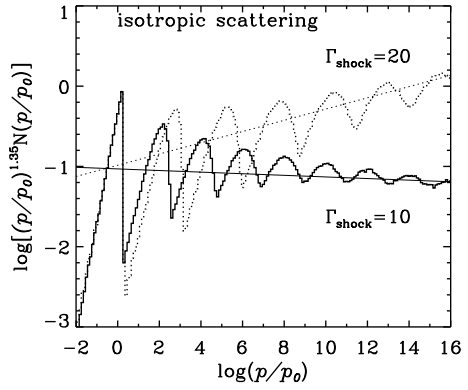

Fig. 5. Momentum spectra obtained from the Monte Carlo simulations (isotropic scattering upstream) for $\Gamma_1 = 10$ (solid curve) and $\Gamma_1 = 20$ (dashed curve) compared with the power-law approximations normalized at the highest momentum.

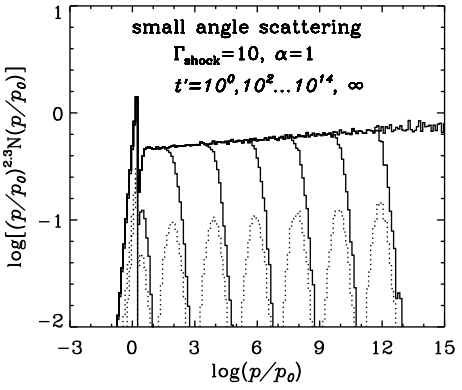

Fig. 6. Momentum spectra obtained from the Monte Carlo simulations (small angle scattering upstream) for $\Gamma_1 = 10$ (upper solid histogram). Spectra at times $t'/t_0^{sc} = 10^0, 10^1, \ldots, 10^{14}$ after injection are also shown for $\alpha = 1$ (lower solid histograms) together with the spectra of particles remaining in the acceleration zone (dotted histograms) at these times.

$a = 360$ for $\Gamma_1 = 20$), the momentum after n cycles is

$p'_n \approx p'_0 a^n$.

The number of particles reaching momentum level p'_n is P_R^n, and a fraction $(1 - P_R)$ of these will escape downstream to contribute to the spectrum of accelerated particles:

$N(> p'_n) = (1 - P_R)P_R^n$.

Since $n = \ln(p'_n/p'_0)/\ln a$, I arrive at

$N(> p'_n) = (1 - P_R)(p'_n/p'_0)^s$

where $s = \ln P_R/\ln a$, giving a differential spectral index $(s - 1) = -1.36$ for $\Gamma_1 = 10$ and $(s - 1) = -1.28$ for $\Gamma_1 = 20$. The differential spectra from the Monte Carlo simulations are compared with the power-law approximations in Fig. 5 and found to agree well (each oscillation results from one acceleration cycle, and at later times these become smeared). Note that if I had used the result of Bednarz and Ostrowskii (1999) for the case of large magnetic field fluctuations ($P_R \sim 0.13$, $a = 1.2\Gamma_1^2$) I would have obtained slightly different spectral indices: $(s - 1) = -1.44$ for $\Gamma_1 = 10$ and $(s - 1) = -1.34$ for $\Gamma_1 = 20$.

In Fig. 6 I show the final spectrum for the small angle scattering case for $\alpha = 1$ and $\Gamma_1 = 10$ for which I find a differential spectrum of -2.28, and for $\Gamma_1 = 20$ (not shown) the index is -2.27. In this figure I also show how the spectrum develops with time after injection, showing separately at each time indicated the spectrum of particles which have escaped, and (dotted curves) the spectrum of particles remaining within the acceleration zone (i.e. not having yet escaped downstream).

6 Summary

I have shown that it is possible to develop "event generators" for rapid and efficient Monte Carlo simulation of the downstream journeys of particles in a simulation of relativistic shock acceleration. By using the event generator described in the accompanying paper (Protheroe 2001), it was possible to obtain good statistics on the spectrum and angular distribution during acceleration over an energy range spanning a factor of 10^{16} in a short time (all the results shown in this paper took less than 90 seconds on an elderly workstation). The Monte Carlo simulation was tested by comparison with estimates of the angular and energy distributions of accelerated particles for the unrealistic case of isotropic scattering both downstream and upstream. Using a simple small angle scattering approximation upstream, results qualitatively in agreement with more sophisticated treatments were obtained.

Acknowledgements. I thank Alina Donea for reading the manuscript. The research of RJP is funded by a grant from the Australian Research Council.

References

Bednarz, J. and Ostrowski, M., Efficiency of cosmic ray reflections from an ultrarelativistic shock wave, Monthly Notices, 310, L11-L13, 1999.

Bednarz, J. and Ostrowski, M., The acceleration time-scale for first-order Feri acceleration in relativistic shock waves, Monthly Notices, 283, 447-456, 1996.

Gallant, Y.A. and Achterberg, A., Ultra-high-energy cosmic ray acceleration by relativistic blast waves, Monthly Notices, 305, L6-L10, 1999.

Kirk, J.G., Schneider, P., Particle acceleration at shocks: a Monte Carlo method, ApJ, 322, 256-265, 1987

Ostrowski, M., Numerical simulations of relativistic shock acceleration, Proc. Rencontres de Moriond 'Very High Energy Phenomena in the Universe', Les Arcs, 2001

Protheroe, R.J., An efficient Monte Carlo scheme for relativistic shock acceleration, these proceedings, 2001.